Theoretical Study of the Gas Phase Decomposition of Glycolic, Lactic, and 2-Hydroxyisobutyric Acids

L. R. Domingo,[†] J. Andrés,[‡] V. Moliner,[‡] and V. S. Safont*[,‡]

Contribution from the Departament de Química Orgànica, Universitat de València, Dr. Moliner 50, 46100 Burjassot, València, Spain, and Departament de Ciències Experimentals, Universitat Jaume I, Box 224, 12080 Castelló, Spain

Received August 14, 1996. Revised Manuscript Received April 21, 1997[⊗]

Abstract: The reaction mechanism associated with the decomposition of three α-hydroxycarboxylic acids (glycolic, lactic, and 2-hydroxyisobutyric) in the gas phase to form carbon monoxide, water, and the corresponding carbonyl compounds has been theoretically characterized by using *ab initio* analytical gradients at the MP2 level of theory with the 6-31G** and 6-31++G** basis sets. A detailed characterization of the potential energy surface points out the existence of three competitive reaction pathways for the decomposition process. The first pathway describes a two-step mechanism, with water elimination and formation of an α-lactone intermediate, achieved by the nucleophilic attack of the carbonylic oxygen atom of the carboxyl group (mechanism A). The second pathway is also a two-step mechanism, but in this case the formation of the α-lactone is obtained by means of the nucleophilic attack of the hydroxylic oxygen atom of the carboxyl group (mechanism B). These two pathways share a common second step in which the α-lactone decomposes. The third pathway is a one-step process in which the decomposition of the corresponding α-hydroxy acid takes place in a concerted fashion (mechanism C). The geometrical parameters of the stationary points appearing along the three pathways and the components of the transition vectors associated to the transition structures calculated using the 6-31G** basis set are similar to those calculated with the larger 6-31G++G** basis set. The decomposition is favorable along pathway A, and the first step can be considered as the rate-limiting step for the global process. The rate constant values for this step increase in the order of glycolic, lactic, and 2-hydroxyisobutyric acids due to the stabilization of the incipient carbocationic center on C_3 with the substitution of hydrogen atoms by methyl groups. The apparent first-order rate constants calculated by transition state theory agree well with the experiments reported by Chuchani and co-workers.

Introduction

The kinetics of the gas phase decomposition of several carboxylic acid derivatives has been experimentally studied by Chuchani and co-workers.[1−5] The results prove the reaction to be homogeneous, to be unimolecular, and to obey a first-order rate law. In particular, the rate constants for the gas phase decomposition at low pressure of the three α-hydroxycarboxylic acids, glycolic (**I**), lactic (**II**), and 2-hydroxyisobutyric (**III**), to form carbon monoxide, water, and the corresponding carbonyl compound has been determined[3] and expressed as a function of temperature by the following Arrhenius-type equations:

$$\underset{\substack{\mathbf{I}\ R_1=R_2=H;\ \mathbf{II}\ R_1=H,\ R_2=CH_3;\\ \mathbf{III}\ R_1=CH_3,\ R_2=CH_3}}{R_1R_2COHCOOH \rightarrow R_1R_2CO + CO + H_2O} \quad (1)$$

$$\log k_{obsd}(s^{-1}) = (14.03 \pm 0.24) - (209.3 \pm 1.5)\ \text{kJ mol}^{-1}\ (2.303RT)^{-1}\ \text{for}\ \mathbf{I} \quad (2)$$

$$\log k_{obsd}(s^{-1}) = (12.24 \pm 0.11) - (182.8 \pm 1.3)\ \text{kJ mol}^{-1}\ (2.303RT)^{-1}\ \text{for}\ \mathbf{II} \quad (3)$$

$$\log k_{obsd}(s^{-1}) = (12.91 \pm 0.13) - (174.7 \pm 1.5)\ \text{kJ mol}^{-1}\ (2.303RT)^{-1}\ \text{for}\ \mathbf{III} \quad (4)$$

Quantum mechanical techniques are used to characterize the potential energy surface (PES) representing a chemical reaction.[6,7] The analysis of PES provides the molecular geometries and vibrational frequencies for reactants, products, intermediates, and transition structures. From these data, the rate constants for the reaction pathways connecting the reactants with the products via the corresponding transition structures can be calculated with practical accuracy. This valuable information can shed some light on the reaction mechanisms, especially in cases where experimental determination is uncertain.

The main aim of this work is the characterization of the reactive PES for the decomposition of the glycolic, lactic, and 2-hydroxyisobutyric acids. The localization of transition structures allows us to determine the corresponding geometries and vibrational frequencies. The calculation of the rate constants for the elementary steps is carried out by means of the transition state theory (TST).[8,9] The theoretical calculations are compared with available experimental results.

* Author to whom correspondence should be addressed.
[†] Universitat de València.
[‡] Universitat Jaume I.
[⊗] Abstract published in *Advance ACS Abstracts,* June 15, 1997.

(1) Chuchani, G.; Rotinov, A. *Int. J. Chem. Kin.* **1989**, *21*, 367.
(2) Chuchani, G.; Domínguez, R. M.; Rotinov, A. *Int. J. Chem. Kinet.* **1991**, *23*, 779.
(3) Chuchani, G.; Martín, I.; Rotinov, A.; Domínguez, R. M. *J. Phys. Org. Chem.* **1993**, *6*, 54.
(4) Chuchani, G.; Martín, I.; Rotinov, A.; Domínguez, R. M.; Pérez, I. M. *J. Phys. Org. Chem.* **1995**, *8*, 133.
(5) Chuchani, G.; Domínguez, R. M. *Int. J. Chem. Kinet.* **1995**, *27*, 85.
(6) Williams, I. H. *Chem. Soc. Rev.* **1993**, 277.
(7) Skancke, P. N. *Acta Chem. Scand.* **1993**, *47*, 629.
(8) Glasstone, K. J.; Laidler, K. J.; Eyring, H. *The Theory of Rate Processes*; McGraw-Hill: New York, 1941.
(9) Laidler, K. J. *Theories of Chemical Reaction Rates*; McGraw-Hill: New York, 1969.

S0002-7863(96)02857-0 CCC: $14.00

Computational Methods

All calculations have been performed with the *GAUSSIAN92/DFT*[10] and *GAUSSIAN94*[11] programs. *Ab initio* calculations including correlation effects have been made by using the MP2 level of theory with the 6-31G**[12] and 6-31++G**[13] basis sets. A recent study on the related system, 2-chloropropionic acid, has shown that this level of theoretical approximation is a reasonable choice and that further enhancements, such as an MCSCF approach with CASSCF treatment, yield very similar results with respect to structural and kinetic parameters.[14]

The Berny analytical gradient optimization routines[15,16] were used for optimization. The requested convergence on the density matrix was 10^{-9} au, and the threshold value of maximum displacement was 0.0018 Å and that of maximum force was 0.00045 hartree/bohr. The nature of each stationary point was established by calculating and diagonalizing the Hessian matrix (force constant matrix). The eigenvalue-following algorithm[17] was used for locating the transition structures. The transition vector (TV)[18] (*i.e.*, the eigenvector associated to the unique negative eigenvalue of the force constants matrix) has been obtained. The intrinsic reaction coordinate (IRC)[19] path was traced in order to check the energy profiles connecting each transition structure to the two associated minima of the proposed mechanism by using the second-order González−Schlegel integration method.[20,21]

Each stationary structure was characterized as a minimum or a saddle point of index 1 by a frequency calculation. The frequency calculations also provide thermodynamic quantities such as zero-point vibrational energy (ZPVE), temperature corrections, and absolute entropies,[22] and consequently, the elementary rate constants can be estimated. These thermodynamic quantities were obtained assuming ideal gas behavior, from the harmonic frequencies and moments of inertia by standard methods.[23] In addition, we have shown[14] that the use of scaled vibrational frequencies at the MP2 level impairs the calculated kinetic parameters; for this reason, the crude *ab initio* frequencies have been used.

The first-order rate constant ($k(T)$) for each first order elementary step of the kinetic scheme (see below) was computed using the TST[8,24] and assuming that the transmission coefficient is equal to 1, as expressed by the following relation

$$k(T) = (kT/h)\exp(-\Delta G^{\ddagger}/RT) \tag{5}$$

which provides a direct relationship between the rate constant for an elementary reaction and its free energy of activation, $\Delta G^{\ddagger}$. In this equation, k and h are the Boltzmann and Planck constants, respectively. $\Delta G^{\ddagger}$ can be calculated from the enthalpy and entropy of activation, as follows:

$$\Delta G^{\ddagger} = \Delta H^{\ddagger} - T\Delta S^{\ddagger} \tag{6}$$

$\Delta S^{\ddagger}$ is the entropy change between the reactants and its corresponding transition structure, and $\Delta H^{\ddagger}$ can be calculated from the following equation

$$\Delta H^{\ddagger} = \Delta E_{\text{elec}} + \Delta E_{\text{ZPVE}} + \Delta(\Delta E_{\text{vib}}(T)) + \Delta E_{\text{rot}}(T) + \Delta E_{\text{trans}}(T) + PV \tag{7}$$

where the six terms on the right are the changes in the electronic energy, in the ZPVE, in the thermal correction to the vibrational energy, in the classical rotational and translational energies, and the work term which is equal to $\Delta n^{\ddagger}RT$.

The absolute entropies were evaluated by the relation[22]

$$S = S_{\text{tr}} + S_{\text{rot}} + S_{\text{vib}} - R\ln\sigma + R\ln m \tag{8}$$

where S_{tr}, S_{rot}, and S_{vib} are the translational, rotational, and vibrational contributions, respectively, R is the ideal gas constant, σ is the rotational symmetry number,[25] and m is the multiplicity of the electronic ground state. A standard pressure of 1 atm was taken in the S calculations.

In spite of the development of improved theories to accurately calculate the rate constants for chemical processes[26] such as RRKM[27,28] or VTST,[29,30] conventional TST[8,9] is still a very useful method to describe chemical reactions, and the molecular mechanism of a given chemical reaction can be understood in terms of transition structure (TS) associated with the chemical interconversion step. We have selected this method to calculate the kinetic parameters in the present study.

Results and Discussion

An extensive exploration of the PESs has been carried out at the MP2/6-31G** level in order to explore the nature of the reaction mechanism for the unimolecular decomposition of the α-hydroxycarboxylic acids. This study considers three competitive reaction pathways. Pathways A and B are stepwise processes; the first step corresponds to the dehydration process with formation of an α-lactone ring, while the second step is associated to the aperture of the α-lactone to yield the corresponding carbonyl compound and the carbon monoxide molecule. Pathway C is a one-step process where the decomposition of the α-hydroxy acids takes place in a concerted fashion. A schematic representation of the variation of the Gibbs free energy for the stationary points is presented in Figure 1. The global process can be schematically described as the following:

$$\mathbf{R} \xrightarrow[-H_2O]{k_1} \mathbf{IN} \xrightarrow[-CO]{k_4} \mathbf{P} \qquad \text{reaction pathway A}$$

$$\mathbf{R} \xrightarrow[-H_2O]{k_2} \mathbf{IN} \xrightarrow[-CO]{k_4} \mathbf{P} \qquad \text{reaction pathway B}$$

$$\mathbf{R} \xrightarrow{k_3} \mathbf{P} + H_2O + CO \qquad \text{reaction pathway C}$$

In Figure 2, the minima reactants (**I**, **II**, and **III** (**R**), α-lactone intermediates (**IN**), and the products (**P**)) for the three mecha-

(10) Frisch, M. J.; Trucks, G. W.; Schlegel, H. B.; Gill, P. M. W.; Johnson, B. G.; Wong, M. W.; Foresman, J. B.; Robb, M. A.; Head-Gordon, M.; Replogle, E. S.; Gomperts, R.; Andres, J. L.; Raghavachari, K.; Binkley, J. S.; Gonzalez, C.; Martin, R. L.; Fox, D. J.; Defrees, D. J.; Baker, J.; Stewart, J. J. P.; Pople, J. A. *GAUSSIAN92/DFT*, Revision G.4; Gaussian, Inc.: Pittsburgh, PA, 1993.

(11) Frisch, M. J.; Trucks, G. W.; Schlegel, H. B.; Gill, P. M. W.; Johnson, B. G.; Robb, M. A.; Cheeseman, J. R.; Keith, T.; Peterson, G. A.; Montgomery, J. A.; Raghavachari, K.; Al-Laham, M. A.; Zakrzewski, V. G.; Ortiz, J. V.; Foresman, J. B.; Cioslowski, J.; Stefanov, B. B.; Nanayakkara, A.; Challacombe, M.; Peng, C. Y.; Ayala, P. Y.; Chen, W.; Wong, M. W.; Andres, J. L.; Replogle, E. S.; Gomperts, R.; Martin, R. L.; Fox, D. J.; Binkley, J. S.; Defrees, D. J.; Baker, J.; Stewart, J. P.; Head-Gordon, M.; Gonzalez, C.; Pople, J. A. *GAUSSIAN94*, Revision B.1; Gaussian, Inc.: Pittsburgh, PA, 1995.

(12) Frisch, M. J.; Pople, J. A.; Binkley, J. S. *J. Chem. Phys.* **1984**, *80*, 3265.

(13) Clark, T.; Chandrasekhar, J.; Spitznagel, G. W.; Schleyer, P. v. R. *J. Comput. Chem.* **1983**, *4*, 294.

(14) Safont, V. S.; Moliner, V.; Andrés, J.; Domingo, L. R. *J. Phys. Chem.* **1997**, *101*, 1859.

(15) Schlegel, H. B. *J. Comput. Chem.* **1982**, *3*, 214.

(16) Schlegel, H. B. *J. Chem. Phys.* **1982**, *77*, 3676.

(17) Tsai, C. J.; Jordan, K. D. *J. Phys. Chem.* **1993**, *97*, 11227.

(18) McIver, J. W., Jr. *Acc. Chem. Res.* **1974**, *7*, 72.

(19) Fukui, K. *J. Phys. Chem.* **1970**, *74*, 4161.

(20) González, C.; Schlegel, H. B. *J. Phys. Chem.* **1990**, *94*, 5523.

(21) González, C.; Schlegel, H. B. *J. Chem. Phys.* **1991**, *95*, 5853.

(22) Hehre, W. J.; Radom, L.; Schleyer, P. v. R.; Pople, J. A. *Ab Initio Molecular Orbital Theory*; John Wiley & Sons: New York, 1986.

(23) McQuarrie, D. *Statistical Mechanics*; Harper & Row: New York, 1986.

(24) Benson, S. W. *The foundations of chemical kinetics*; McGraw-Hill: New York, 1960.

(25) Herzberg, G. *Molecular spectra and molecular structure*; Van Nostrand: Princeton, NJ, 1945; Vol. 2, p 508.

(26) Heidrich, D.; Kliesch, W.; Quapp, W. *Properties of Chemically Interesting Potential Energy Surfaces*; Springer-Verlag: New York, 1991.

(27) Marcus, R. A. *J. Chem. Phys.* **1965**, *43*, 1598.

(28) Forst, W. *Theory of Unimolecular Reactions*; Academic Press: New York, 1973.

(29) Truhlar, D. G.; Garrett, B. C. *Acc. Chem. Res.* **1980**, *13*, 440.

(30) Truhlar, D. G.; Isaacson, A. D.; Garrett, B. *Theory of Chemical Reaction Dynamics*; Chemical Rubber Co.: Boca Raton, FL, 1985.

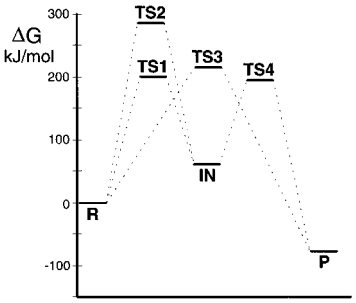

Figure 1. Free energies (kJ/mol) relative to reactants **R** of the stationary points (intermediates, **IN**; transition structures, **TS1**, **TS2**, **TS3** and **TS4**; products, **P**) obtained for the **I** system at the MP2/6-31G** calculation level. The horizontal axis has an arbitrary scale. The energetic difference between **TS1** and **TS3** is larger for the other two systems herein studied.

nisms are sketched. The atom numbering is also indicated. In Figure 3, a representation of the four transition structures corresponding to the three acids is depicted. **TS1** and **TS2** are related to the first step of pathways A and B, respectively. **TS3** appears along the concerted reaction pathway C, and **TS4** is associated to the second and common step of the A and B pathways. The first step of pathways A and B is a dehydration process that takes place by elimination of the hydroxyl group on the C_3 carbon atom. Both reaction pathways differ in how the lactone intermediate is obtained; in pathway A the ring closure is carried out by the attack of the carbonyl oxygen O_4 on the C_3 center, while this nucleophilic process is achieved by the hydroxylic oxygen O_1 of the carboxylic group in the pathway B.

The chirality of the C_3 carbon atom (related with the values of $O_1-C_2-C_3-R_1$ and $O_1-C_2-C_3-R_2$ dihedral angles) in the lactic acid **II** allows for two possible enantiomeric forms for this compound. We have explored both possibilities, and the structures of the stationary points along the corresponding pathways for the two starting enantiomers present identical values of energies, vibrational frequencies, and the remaining geometric parameters. This is not surprising because the Hamiltonian does not contain any part that would disrupt symmetry. We have selected for **II** the configuration shown in Figure 2 in order to avoid calculation of the symmetry-corrected[31,32] values for the variation of the Gibbs free energy that can only take place in system **II**. For system **II**, **IN** and **TS4** corresponding to reaction pathway A are enantiomeric to those belonging to the reaction pathway B.

On the other hand, for systems **I** and **III**, the α-lactones appearing throughout mechanisms A and B are the same compounds (if there is not isotopic distinction between O_1 and O_4). In all cases their corresponding energy and vibrational frequency values are identical, and the k_4 values will be the same for both mechanisms: this is the reason why we do not distinguish between species **IN** and **TS4** appearing along the reaction pathways A and B. In addition, we have carried out a previous analysis in order to find and use the minor energy configurations for the starting reactants.

Energetics. The enthalpy and entropy values for the three reactant models (the three intermediates, the three corresponding products, and the twelve transition structures for reaction pathways A, B, and C) are reported in Table 1.

It should be noted that, according to the results presented in Table 1, the **IN** intermediates (*i.e.*, the respective α-lactones) are appreciably less stable than either **R** or **P**.

The decompositions of the α-hydroxy acids are endothermic processes; ΔH values are positive and decrease in the following order **I** > **II** > **III**.

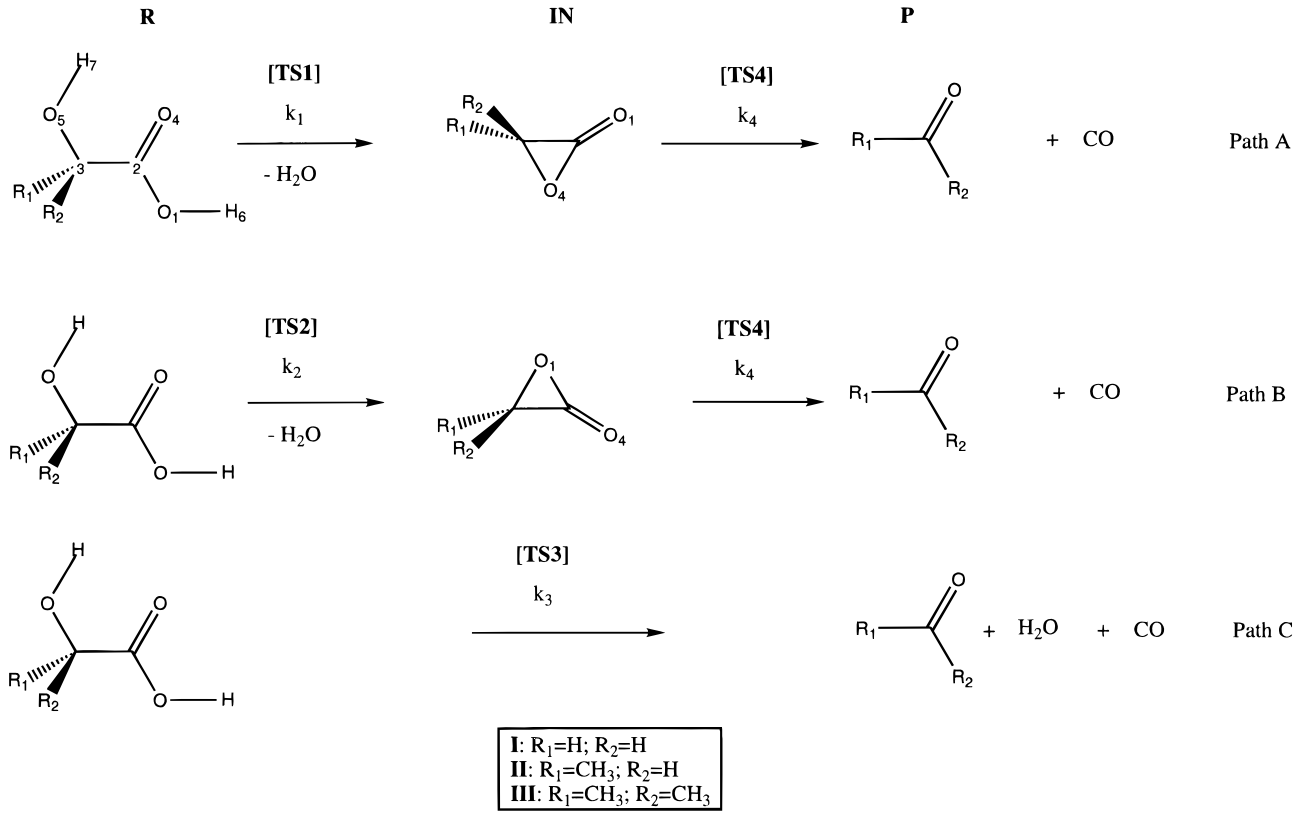

Figure 2. Schematic representation of the minima: reactants **I**, **II**, and **III**, α-lactone intermediates (**IN**), and products (**P**) within the reaction pathways to which they belong. The numbering of the atoms used and the nomenclature for the corresponding rate constants are given. The minimum energy configuration for the systems **I** and **II** is shown for **R**, and for system **III**, the minimum energy configuration involves intramolecular hydrogen bonding between H_6 and O_5. It should be noted that before the corresponding transition structures are attained, for systems **I** and **II**, the intramolecular hydrogen bond must be broken and a rotation around the C_2-C_3 bond takes place. For system **III**, this rotation is not necessary.

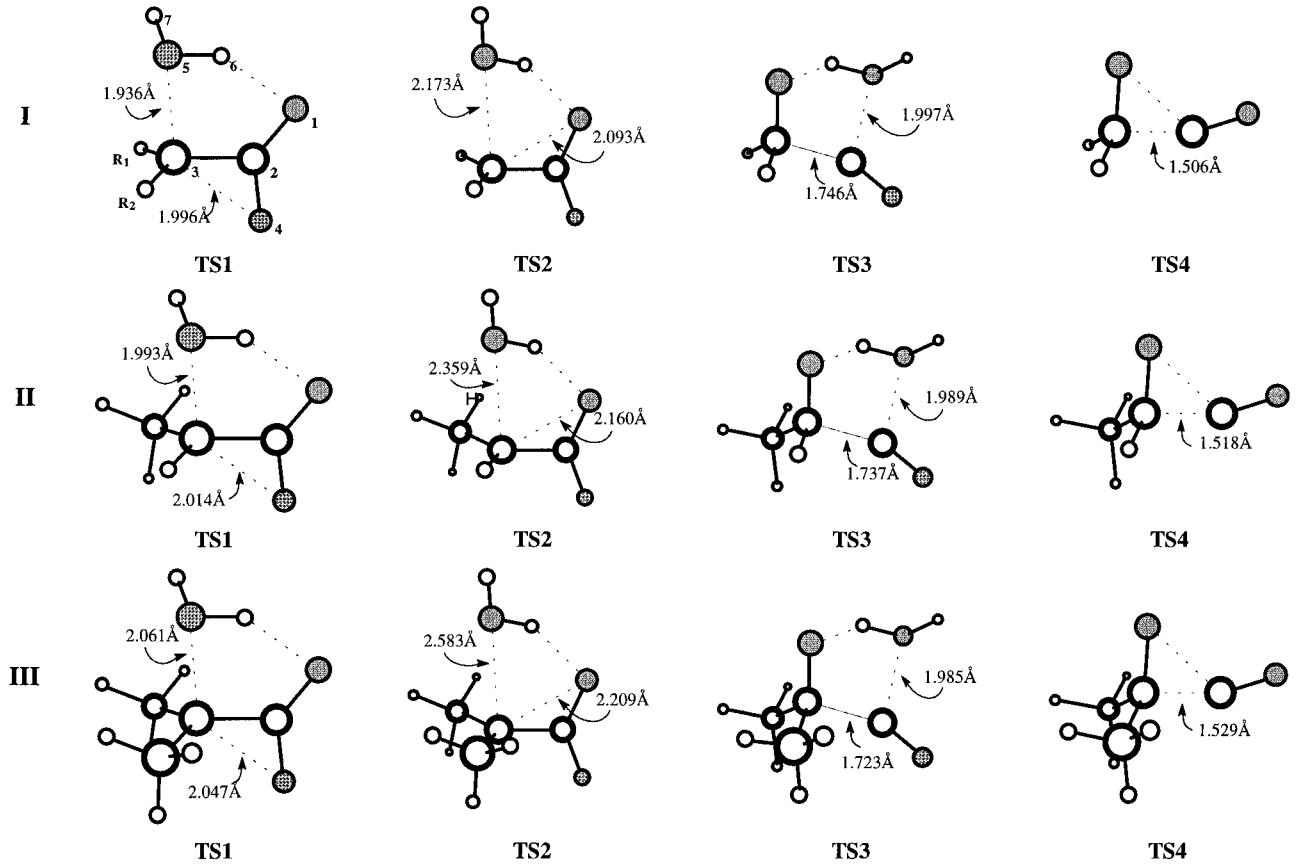

Figure 3. Representation of the four transition structures corresponding to the three acids. **TS1** and **TS2** are related to the first step of the A and B pathways, respectively; **TS3** appear along the C concerted pathway, and **TS4** are associated to the common second step of the A and B pathways.

Kinetic Parameters. The apparent first-order rate constant will be given by

$$k_{ap} = k_1 + k_2 + k_3 \tag{9}$$

A complete analysis of the activation parameters has been carried out at the MP2/6-31G** level. The elementary first-order rate constants k_1, k_2, k_3, and k_4 and the apparent rate constants calculated by means of eq 9, corresponding to the decomposition reactions of the three hydroxycarboxylic acids, are reported in Table 2.

An analysis of the kinetic parameters values for the three reaction pathways shows that the first step of pathway A is favorable with respect to the first step of pathway B and to pathway C. For the three α-hydroxycarboxylic acids, the rate constant values for the first step of pathway A, k_1, are larger than the rate constant values for the first step of pathway B, k_2, and the rate constant value for pathway C, k_3, following the order: $k_1 > k_3 > k_2$. The differences between k_2 and k_1 decrease and the differences between k_3 and k_1 increase when the size of the system increases: The k_2 value can be considered as negligible with respect to k_1 and k_3 values for **I**, but this is not as clear for **II** and of the same order of magnitude as k_3 for **III**. The apparent rate constants values in the three systems are very close to the k_1 value, and in this sense, we can conclude that the step which mainly controls the overall kinetics is the first step of pathway A. On the other hand, the k_4 rate constants are greater than the k_1 or k_2 rate constants; the first step of pathways A and B can then be considered rate-limiting steps within its corresponding path.

A comparison of the values for the calculated apparent rate constants with the experimental results shows quite a good agreement. According to the experimental data,[3] the decomposition rate at 340 °C for **II** is about 3 times that of **I** and the decomposition rate for **III** is *ca*. 66 times that of **I**. Our results at the present calculation level show qualitatively the same trend.

Although the results at the MP2/6-31G** level are good enough for a preliminary discussion of the overall kinetics of the systems, it is desirable to increase the accuracy of the theoretical values. For this purpose, the stationary points (except **P**) have also been optimized at the MP2/6-31++G** level.

The inclusion of diffuse functions yields a decrease of the **TS1**, **TS2**, and **TS3** activation enthalpies (see Table 1), and the corresponding rate constants (k_1, k_2 and k_3) are larger at the MP2/6-31++G** than at the MP2/6-31G** levels (see Table 2). The apparent rate constant value for system **I** is now within the limits of the experimental range, while for systems **II** and **III**, the apparent rate constants present a value of the same order of magnitude as the experimental range (**II**) or its upper limit (**III**).

The increase in the calculation level renders better agreement with experiment, and we again find that the apparent rate constants values are very close to the k_1 value. Thus, the step which mainly controls the overall kinetics is the first step of pathway A. In a previous study on the decomposition of the related system 2-chloropropionic acid,[14] we found that a more sophisticated computational method, MCSCF wave functions with a (6,6) complete active space and the 6-31G** basis set, renders similar energetic values, kinetic parameters, and geometrical variables for the stationary points for this type of decompositions. The results obtained at the MP2 level are acceptable. Additionally, one of the referees notified us that the natural populations in **TS3** for system **I** (where the largest deviations from a single configuration treatment can be expected) are almost exactly 2 or 0, the largest deviation being smaller than 0.0003, in all natural orbitals of this species.

(31) Pechukas, P. *Annu. Rev. Phys. Chem.* **1981**, *32*, 159.
(32) Pollak, E.; Pechukas, P. *J. Am. Chem. Soc.* **1978**, *100*, 2984.

Table 1. Relative Enthalpies (ΔH, kJ/mol) and Relative Entropies (ΔS, J/mol K) to the Corresponding Reactants of the Intermediates, Products, and Transition Structures Calculated at the MP2/6-31G** and MP2/6-31++G** Levels[a]

	MP2/6-31G**		MP2/6-31++G**	
	ΔH	ΔS	ΔH	ΔS
		I		
TS1	222.53	13.92	213.26	13.52
TS2	304.36	31.91	289.42	34.83
IN	165.53	166.64	155.88	165.07
TS3	247.63	32.25	240.73	32.01
TS4	300.08	168.69	278.20	167.11
P	114.57	320.23		
		II		
TS1	207.41	−8.17	198.46	−3.03
TS2	273.01	15.93	251.88	39.47
IN	154.36	146.47	143.96	149.59
TS3	234.68	9.95	228.19	12.99
TS4	284.07	145.59	262.19	148.92
P	94.29	310.36		
		III		
TS1	185.22	−0.17	176.46	4.10
TS2	232.18	30.04	202.87	29.71
IN	138.02	153.26	128.12	155.51
TS3	220.26	11.42	214.17	14.48
TS4	265.16	150.50	244.20	151.75
P	76.79	332.80		

[a] For **IN**, **TS4**, and **P**, the values correspond to the sum of all fragments (*i.e.*, water is summed up for **IN** and **TS4**, while water and carbon monoxide are summed up for **P**), in order to make the comparison with **R** and the other transition structures possible. The ZPVE and temperature corrections are taken into account. For the reactants, total energies calculated at the MP2/6-31G** (au), at 613.15 K are as follows (in parentheses, the values calculated at the MP2/6-31++G** level): glycolic acid (**I**) −303.413445 (−303.439558); lactic acid (**II**) −342.57152 (−342.599622); 2-hydroxyisobutyric acid (**III**) −381.728711 (−381.759365).

Table 2. Theoretically Calculated (at 613.15 K and at the MP2/6-31G** and MP2/6-31++G** levels) First Order Rate Constants (k, s^{-1}) for the Indicated Model Systems and Elementary Steps[a]

	k	
	MP2/6-31G**	MP2/6-31++G**
	I	
k_1	7.51×10^{-6}	4.41×10^{-5}
k_2	6.99×10^{-12}	1.86×10^{-10}
k_3	4.95×10^{-7}	1.86×10^{-6}
k_4	5.64×10^{1}	6.20×10^{2}
k_{ap}	8.01×10^{-6}	4.60×10^{-5}
k_{obsd}	in the range 6.83×10^{-5} to 3.71×10^{-4}	
	II	
k_1	1.02×10^{-5}	1.10×10^{-4}
k_2	4.80×10^{-10}	5.14×10^{-7}
k_3	4.30×10^{-7}	2.21×10^{-6}
k_4	1.02×10^{2}	9.98×10^{2}
k_{ap}	1.07×10^{-5}	1.13×10^{-4}
k_{obsd}	in the range 2.81×10^{-4} to 7.78×10^{-4}	
	III	
k_1	2.08×10^{-3}	1.94×10^{-2}
k_2	7.88×10^{-6}	2.38×10^{-3}
k_3	8.69×10^{-6}	4.14×10^{-5}
k_4	1.35×10^{2}	1.05×10^{3}
k_{ap}	2.10×10^{-3}	2.18×10^{-2}
k_{obsd}	in the range 5.92×10^{-3} to 1.94×10^{-2}	

[a] The apparent rate constants calculated by means of eq 9 (k_{ap}, s^{-1}) and the experimental interval for the observed rate constant (k_{obsd}, s^{-1}) are also included for each system.

Therefore, this result supports the conclusion that a single-configuration treatment may be satisfactory.

Mulliken Population Analysis. Some interesting observations emerge from the Mulliken population analysis.[33] On going from reactant to the transition structure, along the first step of mechanisms A and B, we find that the electronic charge redistribution shows an increasing positive charge developing on the C_3 carbon center. This fact explains the increment of the rate constant value for k_1 and k_2 in the following order: **III** > **II** > **I**. The substitution of the hydrogen atom for electron-releasing methyl groups stabilizes this localized positive charge on the incipient carbocation C_3 center, promoting the dehydration with respect to the ring closure process via mechanisms A and B. From a geometrical point of view, the water elimination is more advanced than the cyclization process at **TS1** and **TS2**. The values of net atomic charges at the C_3 carbon center at **TS1** and **TS2** are 0.01, 0.07, and 0.14 and 0.24, 0.42 and 0.67 au for systems **I**, **II**, and **III**, respectively. These results can explain the larger values of k_1 with respect to k_2. Furthermore, the basicity of the hydroxyl group from primary to tertiary α-hydroxycarboxylic acids increases, making the leaving of this group easier, and as a consequence, an enhancement of the rate constant values is found. These theoretical results agree with the experimental data reported by Chuchani et al.[3]

Table 3. Imaginary Frequency (freq, cm^{-1}), Hessian Unique Negative Eigenvalue (eig, au), Main Components of the Transition Vector (C, au), and Corresponding Geometrical Parameters (G, bonds in angstroms, bond and dihedral angles in deg) and Force Constants (F, au) for **TS1** Corresponding to system **I** Calculated at the MP2/6-31++G** Level

freq	565.93*i*		
eig	−0.071 31		
	C	G	F
C_2-C_3	0.156	1.463	0.756
C_3-O_5	−0.719	1.941	0.047
O_1-H_6	−0.265	1.867	0.213
$O_1-C_2-C_3$	−0.285	127.4	7.585
$C_2-C_3-O_5$	0.164	98.8	6.217
$O_4-C_2-C_3$	0.420	94.1	0.353
$O_1-C_2-C_3-R_1$	0.174	104.9	0.124
$O_1-C_2-C_3-R_2$	−0.169	−102.2	0.122

Table 4. Imaginary Frequency (freq, cm^{-1}), Hessian Unique Negative Eigenvalue (eig, au), Main Components of the Transition Vector (C, au), and Corresponding Geometrical Parameters (G, bonds in angstroms, bond and dihedral angles in deg) and Force Constants (F, au) for **TS2** Corresponding to system **I** Calculated at the MP2/6-31++G** Level

freq	547.75*i*		
eig	−0.192 99		
	C	G	F
C_2-C_3	0.149	1.465	0.736
C_3-O_5	−0.381	2.235	0.029
$O_1-C_2-C_3$	0.506	101.6	11.856
$C_2-C_3-O_5$	−0.356	110.7	9.040
$O_4-C_2-C_3$	−0.511	123.3	0.310
$H_6-O_1-C_2$	−0.366	113.2	3.939
$O_1-C_2-C_3-R_2$	0.105	−92.9	0.089
$O_1-C_2-C_3-R_1$	−0.124	97.8	0.090

Geometries and Transition Vectors. In Tables 3−6, the TV and the geometries for **TS1**, **TS2**, **TS3**, and **TS4** are reported for the **I** system and the MP2/6-31++G** calculation level. For the other systems and calculation levels, the results are reported as Supporting Information. The theoretical results confirm that the first step for mechanisms A and B is the dehydration processes with the formation of the corresponding α-lactone intermediate via **TS1** and **TS2**, respectively. These transition structures can be described as distorted five-membered rings (formed by the C_3, C_2, O_1, H_6, and O_5 atoms with participation of the O_4 oxygen atom for **TS1**). The second step

(33) Mulliken, R. S. *J. Chem. Phys.* **1955**, *23*, 1833.

Table 5. Imaginary Frequency (freq, cm^{-1}), Hessian Unique Negative Eigenvalue (eig, au), Main Components of the Transition Vector (*C*, au), and Corresponding Geometrical Parameters (*G*, bonds in angstroms, bond and dihedral angles in deg) and Force Constants (*F*, au) for **TS3** Corresponding to system **I** Calculated at the MP2/6-31++G** Level

freq		512.51*i*	
eig		−0.080 26	
	C	*G*	*F*
C_2-O_1	−0.547	2.034	0.027
C_2-C_3	−0.647	1.714	0.047
C_3-O_5	0.182	1.296	0.549
O_1-H_7	0.352	1.040	0.209
$C_2-C_3-R_1$	0.132	96.7	0.330
$O_4-C_2-C_3$	−0.138	152.9	0.165
$H_7-O_1-C_2$	−0.129	84.3	0.248
$C_2-R_1-C_3-R_2$	−0.212	−100.1	0.203

Table 6. Imaginary Frequency (freq, cm^{-1}), Hessian Unique Negative Eigenvalue (eig, au), Main Components of the Transition Vector (*C*, au), and Corresponding Geometrical Parameters (*G*, bonds in angstroms, bond and dihedral angles in deg) and Force Constants (*F*, au) for **TS4** Corresponding to system **I** Calculated at the MP2/6-31++G** Level

freq		528.00*i*	
eig		−0.100 67	
	C	*G*	*F*
C_2-C_3	−0.442	1.500	0.191
C_3-O	0.225	1.340	0.492
C_3-C_2-O	−0.528	88.4	0.209
$O'-C_2-C_3$	0.571	162.1	0.146
$C_2-C_3-R_2$	0.235	108.8	0.219
$C_2-C_3-R_1$	0.235	108.8	0.219
$C_3-O-C_2-R_2$	0.135	−120.8	0.235
$C_3-O-C_2-R_1$	−0.135	120.8	0.235

for both mechanisms is the ring opening, leading to carbon monoxide and the corresponding carbonyl compound via **TS4**.

On the basis of their experimental data, Chuchani et al.[3] have proposed a transition structure that corresponds to **TS2** of the mechanism B. Our theoretical results point to mechanism A, via **TS1**, as the favorable reaction pathway for the decomposition process. The nucleophilic attack on C_3 is mainly achieved by the carbonylic oxygen atom.

Geometrical parameters calculated for the transition structures using the MP2/6-31G** are similar to those calculated with the larger basis set. Thus, the bond distances differ by up to 7%, the bond angles differ by up to 4.2%, and the dihedral angles by up to 5.6%. The maximum discrepancies are always found for **TS2** of system **II** and correspond to the C_3-O_5 bond distance, the $O_4-C_2-C_3$ bond angle, and the $O_1-C_2-C_3-R_1$ dihedral angle. The same can be assessed with respect to the TV components, which can be considered as qualitatively invariant to the inclusion of diffuse functions, except for the components corresponding to **TS2** of systems **II** and **III**, where significative variations are found between the weight of the components corresponding with the C_2-C_3 and C_3-O_5 distances.

For **TS1**, the TV is similar for the α-hydroxycarboxylic acids **I**, **II**, and **III**, the main components of TV being the C_3-O_5 and O_1-H_6 distances and the $O_4-C_2-C_3$ and $O_1-C_2-C_3$ bond angles. The distances are associated to the dehydration processes: the O_1-H_6 distance corresponds to the hydrogen transfer from O_1 to O_5 oxygen atoms, the C_3-O_5 distance is a measure of the bond-breaking process, the $O_4-C_2-C_3$ bond angle is related to the nucleophilic attack of the O_4 atom on C_3 center with formation of the α-lactone ring, and the $O_1-C_2-C_3$ bond angle is related to the motion of O_1, which is moving away from C_3. The largest component of TV corresponds to the C_3-O_5 distance (around 50%). Following the order of **I**, **II**, and **III**, the values calculated at the MP2/6-31++G** level show that the C_3-O_5 distance increases from 1.941 to 2.079 Å, the $O_4-C_2-C_3$ bond angle increases from 94.1° to 96.9°, and the O_1-H_6 distance decreases from 1.867 to 1.754 Å. The value of $O_1-C_2-C_3$ bond angle does not vary appreciably with the change of the system size. The electron-releasing effect of the methyl group on C_3 indicates that the C_3-O_5 bond-breaking process is advanced while the nucleophilic attack, related to the $O_4-C_2-C_3$ bond angle, and the hydrogen transfer from O_1 to O_5, related to the O_1-H_6 distance, suffers a delay along the reaction pathway.

For **TS2**, the dominant components of the TV are the C_3-O_5 distance and the $O_1-C_2-C_3$, $C_2-C_3-O_5$, $O_4-C_2-C_3$, and $H_6-O_1-C_2$ bond angles. The distance is associated with the dehydration process, the $O_1-C_2-C_3$ bond angle corresponds to the nucleophilic attack of the O_1 oxygen atom on C_3 center, and the three remaining geometrical variables are involved in both processes. The values calculated at the MP2/6-31G** level render increases in the C_3-O_5 distance from 2.235 to 2.751 Å and in the values of the $O_1-C_2-C_3$ bond angle from 101.6° to 109.7° in the order of **I**, **II**, and **III**. This behavior is explained following arguments on methyl substitution similar to those used for **TS1**. A comparison of the values of the C_3-O_5 bond in **TS1** and **TS2** shows that the breaking process of this bond is more advanced in **TS2,** while an analysis of the values for $O_1-C_2-C_3$ and $O_4-C_2-C_3$ bond angles in both stationary points shows a more advanced nucleophilic attack of O_1 or O_4 on C_3 center for mechanisms A and B, respectively, in **TS1** than in **TS2**. The dehydration and the nucleophilic attack processes take place on the same side, along the axis defined by the C_2-C_3 bond for the mechanism B, while they occur on opposite sides in mechanism A. This explains the lower energy for **TS1** with respect to **TS2**.

For **TS3**, there are internal variables that always participate significantly in the TV: the C_2-O_1 and C_2-C_3 bond-breaking and the O_1-H_7 bond-forming processes and, to a lesser extent, the C_3-O_5 distance, that changes from a single to a double bond. This reaction pathway corresponds to a concerted mechanism. The geometry and transition vector components are weakly dependent on the methyl substitution on C_3 atom.

A comparison between the three alternative mechanisms shows that, in **TS1** and **TS2**, the hydrogen atom transferred is the H_6 atom, which moves from O_1 (the carboxyl group) to O_5 (the hydroxyl group) atoms, while in **TS3** the hydrogen atom transferred is the H_7 atom, moving from O_5 atom to O_1 atom. The pK_a of the COOH group is *ca.* 4.8 while the pK_a of OH group is ca. 16.0. Thus, in order to avoid the excess of negative charge associated with the O_5-H_7 bond-breaking process that can be developed within the mechanism C on O_5 oxygen atom, a concerted fragmentation involving the O_1, C_2, C_3, O_5, and H_7 centers occurs.

For **TS4**, the internal variables that participate significantly in the TV are the C_2-C_3 bond-breaking, the C_3-O_4 or C_3-O_1 distance that evolves from single to double bond (represented in Table 6 and in Supporting Information by C_3-O), and the $C_3-C_2-O_4$ or $C_3-C_2-O_1$ and $O_1-C_2-C_3$ or $O_4-C_2-C_3$ bond angles (represented by C_3-C_2-O and $O'-C_2-C_3$, respectively, where O′ is the oxygen atom that will form part of the carbon monoxide molecule at the end of mechanisms A and B). These reaction pathways correspond to the ring opening of the α-lactone with formation of the carbon monoxide molecule and the corresponding carbonyl compound.

Table 7. Pauling Bond Orders (BO) and Percentage of Evolution of the Bond Order through the Chemical Step (% Ev) Calculated by Means of Eqs 10 and 11, respectively[a]

	BO			% Ev		
	I	**II**	**III**	**I**	**II**	**III**
			TS1			
C_3-O_5	0.17	0.14	0.13	83.0	85.6	87.5
C_3-O_4	0.22	0.20	0.21	17.2	15.1	16.0
O_1-H_6	0.06	0.07	0.07	98.2	97.2	96.3
C_2-O_1	1.43	1.44	1.41	67.9	69.3	66.3
C_2-O_4	1.28	1.29	1.30	44.5	42.3	44.5
			TS2			
C_3-O_5	0.08	0.04	0.02	92.3	95.8	97.8
C_3-O_1	0.16	0.13	0.12	10.2	7.3	5.9
O_1-H_6	0.06	0.05	0.05	98.3	98.5	98.7
			TS3			
C_2-O_1	0.12	0.12	0.12	88.5	88.2	88.1
C_2-C_3	0.45	0.47	0.53	54.6	52.6	47.3
C_3-O_5	1.49	1.48	1.55	57.3	54.5	53.8
O_5-H_7	0.20	0.21	0.23	80.3	78.8	77.2
O_1-H_7	0.19	0.21	0.22	19.3	20.7	21.8
			TS4			
C_2-C_3	0.83	0.80	0.77	17.3	20.5	22.9
C_3-O	2.01	2.09	2.15	53.5	54.9	55.8
C_2-O	0.12	0.12	0.12	87.8	87.6	87.6

[a] For **TS4**, C_3-O represents the C_3-O_4 double bond formation for the A pathway or the C_3-O_1 double bond formation for the B pathway, while C_2-O represents the C_2-O_4 bond breaking for the A pathway or the C_2-O_1 bond breaking for the B pathway. The results were obtained from the MP2/6-31G** calculations.

The imaginary frequency values are in the range of 476−579*i*, 299−589*i*, 512−631*i*, and 511−580*i* cm^{-1} for **TS1**, **TS2**, **TS3,** and **TS4**, respectively; these stationary points are associated with the heavy atom motions. The force constants are all positive, and the negative eigenvalue arises from the cross-terms off-diagonal of the Hessian matrix.

Bond Order Analysis. A more balanced measure of the extent of bond forming or bond breaking along a reaction pathway is provided by the concept of bond order (BO). This theoretical tool has been used to study the molecular mechanism of chemical reactions.[34−37] To follow the evolution of the three alternative mechanisms, Pauling bond orders[38] (BO) were calculated for the different stationary points through the following expression

$$\mathrm{BO} = \exp[(R(1) - R(\mathrm{SP})/0.3] \qquad (10)$$

where R(SP) represents the bond length in the stationary point (SP) considered and R(1) represents the reference bond length. The reference values considered for the bonds that are being broken or that evolve from single to double bonds in each elementary step were the equilibrium distances at the beginning of the step (*i.e.*, at **R** or **IN**). For the bonds that are being formed, or that evolve from double to single bonds, the reference values were the equilibrium distances at the end of the step (*i.e.*, at **P** or **IN**). The results are presented in Table 7.

With this choice of reference bond lengths, the bond order of a single bond will always be 1. However, due to the form of eq 10, the calculated bond order can be distinct from 0 for a distance which is not a bond, or distinct of 2 for a double bond. It is more explicit to use the percentage of evolution of the bond order through the chemical step, calculated by means of

$$\%\mathrm{Ev} = \frac{\mathrm{BO(TS)} - \mathrm{BO}(R)}{\mathrm{BO}(P) - \mathrm{BO}(R)} \times 100 \qquad (11)$$

where BO(TS) is the calculated bond order at the corresponding transition structure and BO(R) and BO(P) are the calculated bond orders at the stationary points located at the beginning and the end of each elementary step, respectively. The results are also included in Table 7.

From the values reported in this table, the C_3-O_5 and O_1-H_6 bond-breaking processes, associated to the dehydration, are more advanced than the C_3-O_4/C_3-O_1 bond-forming processes, corresponding to the nucleophilic attack on the C_3 center in **TS1** and **TS2**. The water elimination has progressed more than the cyclization process along the reaction pathways of mechanisms A and B. The change of the bond order in the C_2-O_1 and C_2-O_4 distances for **TS1** is slightly asynchronous, the double bond formation (C_2-O_1) being more developed than the transformation from double to single bond in C_2-O_4.

In **TS3**, the progress of the reaction can be measured by the change of the following variables: the C_2-O_1 distance, corresponding to the water elimination in this mechanism, the O_5-H_7 and the O_1-H_7 distances, associated to the H_7 transfer from O_5 to O_1 atoms, the C_2-C_3 distance, corresponding to the leaving of carbon monoxide, and the C_3-O_5 distance that changes from single to double bond. An analysis of the data reported in Table 7 shows that the dehydration process (C_2-O_1 and O_5-H_7 bond distances) is more advanced than the C_2-C_3 bond-breaking process with the formation of the corresponding carbonyl compound. The H_7 atom has broken its original bond with O_5 up to 80%, but the formation of the O_1-H_7 bond has progressed only up to 22%. The molecular mechanism corresponds to an asynchronous concerted fragmentation process, and the transferring hydrogen atom has some proton-like character, as can also be assessed from an analysis of the Mulliken population.

In **TS4**, the progress of the reaction can be measured by the change of the following bonds: the C_2-C_3 distance, related to the carbon monoxide elimination, the C_3-O distance, which changes from a single to double bond, and the C_2-O distance corresponding to the aperture of the α-lactone ring. An analysis of the data reported in Table 7 shows that the aperture process of the α-lactone ring and the formation of the double bond C_3-O are more advanced than the elimination of carbon monoxide. It must be noted that the calculated bond order for the last distance is greater than 2; the calculated bond order at products (where the bond is a double bond) for this distance is *ca* 3.0, thus reflecting the convenience of the use of eq 11 instead of simply eq 10.

Conclusions

Extensive *ab initio* explorations of multidimensional PES, reported in this work, were performed with the intention of developing a better understanding of the elimination kinetics of carboxylic acid derivatives in the gas phase. The reaction mechanisms for the decomposition of glycolic, lactic, and 2-hydroxyisobutyric acids have been investigated with the use of the MP2/6-31G** and the MP2/6-31G++G** calculation levels. Following the results obtained for the decomposition of 2-chloropropionic acid,[14] the inclusion of the correlation energy at the MP2 level is necessary to obtain an accurate calculation of the kinetic parameters. The stationary points on the relevant PESs were localized and characterized by the gradient technique. The first-order rate constants for the decomposition processes were evaluated in terms of the TST.

(34) Varandas, A. J. C.; Formosinho, S. J. F. *J. Chem. Soc., Faraday Trans. 2* **1986**, 282.
(35) Lendvay, G. *J. Mol. Struct. (THEOCHEM)* **1988**, *167*, 331.
(36) Lendvay, G. *J. Phys. Chem.* **1989**, *93*, 4422.
(37) Lendvay, G. *J. Phys. Chem.* **1994**, *98*, 6098.
(38) Pauling, L. *J. Am. Chem. Soc.* **1947**, *69*, 542.

The theoretical results have been compared with experimental data. According to the results obtained at this level, the conclusions can be summarized as follows:

(i) A detailed characterization of the PESs points out the existence of three competitive reaction pathways for the decomposition process of α-hydroxy acids. Four transition structures and one intermediate have been characterized.

(ii) The geometrical parameters of these stationary points and the components of the TV of the transition structures calculated using the MP2/6-31G** basis set are similar to those calculated with the larger MP2/6-31G++G** basis set.

(iii) An analysis and comparison of the calculated and experimental rate constants show that the decomposition is favorable along a two-step mechanism. The first and rate-limiting step of the global process is associated to the water elimination with formation of an α-lactone intermediate, by means of the nucleophilic attack carried out by the carbonyl oxygen atom. This process is associated with the polarization of the C−OH bond of the hydroxyl group with subsequent dehydration by assistence of the acidic H of the COOH. The corresponding transition structure is a deformed five-membered ring. The process is followed by an opening of the intermediate ring to obtain carbon monoxide and the corresponding carbonyl compound.

(iv) The water elimination is more advanced than the cyclization process at the transition structure associated with the first and rate-limiting step for the stepwise mechanism.

(v) The substitution of a hydrogen atom for an electron-releasing methyl group stabilizes the localized positive charge on the incipient carbocationic center, promoting the decomposition process. Furthermore, the basicity of the hydroxyl group from primary to tertiary α-hydroxycarboxylic acids increases, making the leaving of this group easier and as a consequence an enhancement of the rate constant values in the order 2-hydroxyisobutyric acid > lactic acid > glycolic acid is found. This theoretical result agrees with experimental data.

(vi) The validity of the theoretical results is determined by comparing the calculated rate constants with the observed values (experimental data). The inclusion of diffuse functions improves the results, and a quantitative agreement is achieved between the theoretical and experimental results.

(vii) A comparison of the mechanism of the decomposition of 2-hydroxycarboxylic acids and 2-chloropropionic acid[14] shows that pathway A is the most favorable channel for this type of chemical reactions. However, is important to note that pathway C can be partially rate-limiting, depending on the conditions (different temperature and pressure values).

Acknowledgment. This work was supported by research funds provided by the Ministerio de Educación y Ciencia of the Spanish Government by DGICYT (project PB93-0661). All calculations were performed on two Silicon Graphics Power Challenge L, belonging to the Servei d'Informàtica of the Universitat Jaume I. We are most indebted to this center for providing us with computer facilities. The final version of this paper has been substantially improved by the comments and criticisms raised by three referees. We respectfully express our indebtedness to them.

Supporting Information Available: Tables giving the imaginary frequency, Hessian unique negative eigenvalue, and main components of TV, corresponding geometric parameters and force constants for **TS1**, **TS2**, **TS3**, and **TS4** corresponding to systems **I**, **II**, and **III**, calculated at the MP2/6-31G** level, and to systems **II** and **III**, calculated at the MP2/6-31++G** level, table giving the full geometries for the stationary points found at the MP2/6-31G** level, and table giving the Arrhenius activation energies and preexponential factors for the different chemical steps (12 pages). See any current masthead page for ordering and Internet access instructions.

JA962857V